Role of electron and hole trapping in the degradation and breakdown of SiO_2 and HfO_2 films

D. Z. Gao,[1] J. Strand,[1] A.-M. El-Sayed,[1] A. L. Shluger[1]
[1]Department of Physics and Astronomy, UCL, Gower Street, London WC1E 6BT, UK

A. Padovani[2] and L. Larcher[3]
[2]MDLab, Via Sicilia, 31, 42122 Reggio Emilia RE, Italy
[3]DISMI, University of Modena and Reggio Emilia, Via Amendola 2, 41122 Reggio Emilia (RE), Italy

***Abstract*—We investigated possible mechanisms for correlated defect production in amorphous (a) SiO_2 and HfO_2 films under applied stress bias using *ab initio* simulations. During bias application, electron injection into these films may lead to the localization of up to two electrons at intrinsic trapping sites which are present due to the natural structural disorder in amorphous structures. Trapping two electrons weakens Si-O and Hf-O bonds to such an extent that the thermally activated creation of Frenkel defects, O vacancies and O^{2-} interstitial ions, becomes efficient even at room temperature. Bias application affects defect creation barriers and O^{2-} interstitial diffusion. The density of trapping sites is different in a-SiO_2 and a-HfO_2. This leads to qualitatively different degradation kinetics, which results from different correlation in defect creation in the two materials. These effects affect TDDB statistics and its dependence on the film thickness.**

***Keywords*- Amorphous SiO_2, HfO_2; Dielectric breakdown; Defect creation; DFT calculations; Electron traps.**

I. Introduction

Under an applied stress bias, field-effect transistors (FETs) experience gradually increasing gate leakage, noise signal, V_T shift, decrease of trans-conductance, and other degradation effects, which are accelerated by strong bias and may lead to dielectric breakdown. These effects have generally been attributed to defect generation and aggregation in the gate stacks [1]. The creation of new defects is associated with structural changes in the oxide, which requires significant energy [2]. In particular, the aggregation of oxygen vacancies as a result of electrically stressing sub-stoichiometric amorphous SiO_x (x=1.3–2) films is thought to facilitate the dielectric breakdown of complementary metal-oxide-semiconductor (CMOS) devices [3] and electroforming in ReRAM cells [4-7]. However, the fundamental atomistic mechanisms behind these processes are still poorly understood. Both the creation of additional oxygen vacancies [4,6,8] and the clustering of diffusing vacancies [5,7] have been proposed as mechanisms for vacancy aggregation.

Recent simulations [9,10] shed some light on the feasibility of such mechanisms. Computational modelling was used to investigate the structures and binding energies of vacancy dimers and trimers in a-SiO_2, the energy barriers for the diffusion of individual vacancies, and whether this diffusion can be stimulated by the trapping of injected electrons at vacancies [9]. The calculations of di- and tri-vacancy clusters demonstrate that there are favourable sites for vacancy aggregation in a-SiO_2 with maximum binding energies of approximately 0.13 eV and 0.18 eV, respectively. However, an average neutral vacancy diffusion barrier was calculated to be about 4.6 eV, rendering the clustering of randomly distributed neutral vacancies unfeasible.

Calculations performed for monoclinic HfO_2 [10] demonstrate that formation of neutral oxygen vacancy aggregates is accompanied by small energy gain, which depends on the size and shape of the aggregate. In the most strongly bound configurations, vacancies are unscreened by Hf cations and form voids within the crystal, with the larger aggregates having larger binding energy per vacancy (0.11 to 0.18 eV). The negatively charged di-vacancy was found to have similar binding energies to the neutral one, while the positively charged di-vacancy was found to be unstable. Thus, aggregation process of either neutral or negatively charged oxygen vacancies in m-HfO_2 is energetically feasible. However, the energy barrier for the diffusion of neutral O vacancies is about 2.4 eV, again suggesting that aggregation of vacancies via diffusion processes is too slow to explain electroforming in HfO_2 films.

The realization that the formation of oxygen vacancy clusters in a-SiO_2 and m-HfO_2 via thermally activated diffusion is inefficient suggests that an alternative mechanism is responsible for the aggregation of oxygen vacancies under electrical bias. Ambiguities in proposed physical mechanisms for the generation of structural defects under the stress conditions and the partial reversibility of degradation point to a possibility that the stress-induced instability might be primarily caused by creation and recombination of Frenkel defects.

In this paper, we briefly review the mechanisms of Frenkel defect creation in a-SiO_2 and a-HfO_2 at zero bias and facilitated by electron injection and discuss the feasibility of such mechanisms in explaining the breakdown and electroforming processes in a-SiO_2 and a-HfO_2 films. We propose mechanisms that can produce new vacancies near pre-existing vacancies in a-SiO_2 and a-HfO_2. Two electrons trapped at a pre-exiting vacancy facilitate the formation of a new vacancy and an interstitial O^{2-} ion. However, the energy barriers for defect creation in a-SiO_2 are much lower than those in a-HfO_2, whereas the density of electron trapping sites in a-HfO_2 is much higher than in a-SiO_2. These results suggest that

correlation effects in the time to breakdown statistics of a-SiO_2 and a-HfO_2 films should be different.

II. METHODS OF CALCULATIONS

The initial models of a-SiO_2 and a-HfO_2 structures were created using classical forcefields [11,12] and the LAMMPS package [13]. Nine periodic models of a-SiO_2 and a-HfO_2, each containing 216 and 324 atoms, respectively, were generated using classical molecular dynamics and a melt and quench procedure in an NPT ensemble. The volume and geometry of these structures were then fully optimized using density functional theory (DFT) as implemented in the CP2K code [14-20] with the range-separated hybrid PBE0-TC-LRC functional [21] and an exchange cutoff radius of 4.0 Å. All calculations were performed in the Γ point of the Brillouin zone. These calculations and the amorphous structures are described in detail in [8,9, 22,23].

Briefly, the densities of the DFT optimized a-SiO_2 structures used in this work were 2.1-2.2 g cm^{-3} and those for a-HfO_2 were in the range of 9.6-9.7 g cm^{-3}. The a-SiO_2 structures were found to form continuum random networks of tetrahedra with distributions of Si-O bond lengths, O-Si-O angles, and Si-O-Si angles in good agreement with experiment [22]. All Si atoms were initially 4-coordinated, and all O atoms were 2-coordinated. The calculated average one-electron Kohn-Sham (K-S) band gap was 8.1 eV.

In contrast, a-HfO_2 samples are characterized by the distributions of Hf and O ion coordination and bond lengths [23]. In particular, around 56% of the Hf atoms are bonded to 6 oxygen atoms, 38% are bonded to 7 oxygen atoms, and 6% to 5 oxygen atoms. On the other hand, 83% of the oxygen atoms are 3 coordinated and 6% of oxygen atoms are 2 coordinated. The band gaps of these initial structures did not contain localized states due to under-coordinated atoms and 6.0 eV on average (ranging from 5.8 to 6.2 eV in different structures). We note that a more detailed comparison of band gap energy with experiment in amorphous systems involves defining a mobility edge, which is beyond the scope of this paper and is discussed in detail in a separate publication [24].

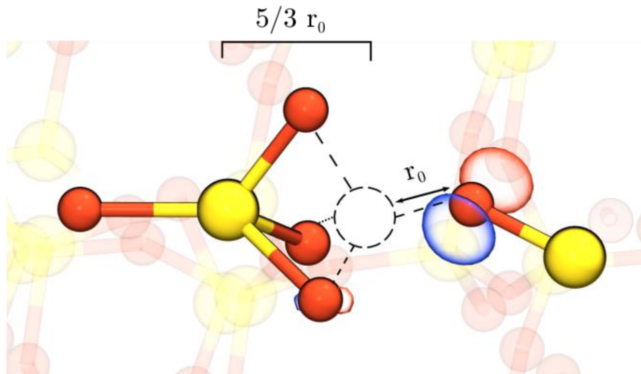

Figure 1. Schematic of Si–O dissociation in a-SiO_2. Si atoms are drawn in yellow while O atoms are red. The Si atom drawn on the left side has displaced through the plane of its neighbors and weakly interacts with the highlighted back oxygen atom. Its original position and Si–O bonds are highlighted as dashed circles and lines respectively. The Si atom has moved approximately 5/3 r_0 through the plane of its neighbors, where r_0 is the length of the original Si--O bond which is also labeled in the figure.

III. BREAKING SI-O BONDS: THE ROLE OF BIAS

Previous studies [25] suggest that bias application can break Si–O bonds in a-SiO_2. To test this assertion, we performed DFT calculations for two models of bond breaking in a-SiO_2. First, we used a model proposed in [26,27]. In these studies, the Si–O bond was described in a cluster of two SiO_4 tetrahedra using an extended Mie-Grüneisen model. The bond energy of Si–O was calculated to be ~5.4 eV and it was shown that displacing the central Si ion of a SiO_4 tetrahedron through the plane of three of its oxygen neighbors (see Fig. 1) resulted in a local minimum. According to previous calculations using a cluster model [27], this occurs when a Si–O bond is extended to 2.83 Å or about 5/3 of the equilibrium Si–O bond length of 1.7 Å.

We used DFT to calculate the same process in a periodic a-SiO_2 model described above, which accounts for all interactions in an extended network. Starting from an equilibrium structure, a single Si–O bond was stretched from 1.61 to 2.68 Å. This involved displacing a Si atom through the plane of three of its O neighbors, as shown in Fig. 1. However, we found that the resulting defect pair was unstable and recombined spontaneously in all geometries used. Thus, this mechanism does not provide a feasible reaction path for Si–O bond dissociation.

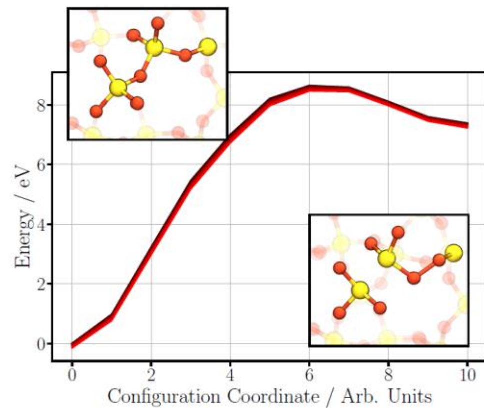

Figure 2. The potential barrier for forming the Frenkel-like defect in α-quartz. The x-axis is the configuration coordinate of the Frenkel defect generation while the y-axis shows the system's total energy. The left and right insets show the atomic structures of the initial and final configurations, respectively. Multiple lines are shown in this plot. The red lines, which are always lower in energy, illustrate the barrier when an electric field is applied.

Another possible mechanism for Si–O dissociation is the formation of a Frenkel defect pair where an O ion is displaced from its typical position in a-SiO_2 structure into an interstitial position leaving behind an O vacancy. We generated this configuration by displacing an O ion from its bridging configuration towards an interstitial position followed by a geometry optimization. This created a stable nearest neighbor pair of Frenkel defects: a neutral O vacancy with a Si–Si bond of 2.35 Å and a peroxy bridge Si–O–O–Si configuration shown in Fig. 2. The energy of this defect pair is 7.4 eV higher than that of bulk a-SiO_2. The calculated energy barrier to displace

the O in this manner and create Frenkel defects is 8.52 eV (see Fig. 2). The recombination barrier for O to return from the interstitial position back to its bridging position and healing the defect is 1.14 eV.

To test the idea [25-27] that an electric field can significantly reduce such barriers, we performed DFT calculations with the application of an electric field of different strength along the O ion displacement path using the modern theory of polarization and the so-called Berry phase method [28]. Application of a field reduces the barrier in a linear fashion, even when using strong fields. The lowest curve in Fig. 2 shows the potential energy of the Frenkel defect pair generation mechanism at the strongest field of 10 $MVcm^{-1}$. The calculated barrier reduction of only 0.065 eV shows that barriers for this process are affected negligibly by the application of an electric field. These results demonstrate clearly that an applied external field would not accelerate this type of Si–O dissociation and vacancy creation and that alternate mechanisms need to be considered.

IV. Role of electron injection

Several previous studies have suggested that electron injection into the oxide resulting from bias application can facilitate the formation of Frenkel defects in monoclinic [29] as well as amorphous [30] HfO_2 and in a-SiO_2 [8]. Here we focus on amorphous SiO_2 and HfO_2. In both materials, the structural disorder leads to formation of precursor sites for electron trapping. However, the structure, density and properties of these sites are quite different. In a-SiO_2, trapping sites correspond to wide O-Si-O angles (>132°) in the otherwise continuous random network a-SiO_2 structure [22]. They can accommodate up to two electrons in the states localized on one Si atom and located about 3.2 eV below the bottom of the SiO_2 conduction band. The density of electron traps was estimated at $4{\cdot}10^{19}$ cm^{-3} [22].

In a-HfO_2 structural disorder, such as under-coordinated ions and elongated bonds, serve as precursor sites for electron trapping [23]. These sites can also accommodate up to two electrons. In an electron polaron, the extra electron is localized around 2 or 3 Hf atoms. The bi-polaron formation causes strong Hf–O bond weakening manifested in significant (about 0.3 Å) ionic displacements. The K-S energy levels of the polaron states in a-HfO_2 are also much deeper than in m-HfO_2, and are located 2.24 eV below the bottom of the conduction band, on average. The density of electron trapping sites is much higher than in a-SiO_2 with an average distance between them of about 8 Å that results in a density of $\sim 2{\cdot}10^{21}$ cm^{-3} [23].

The formation of bi-polaron states in both cases leads to the elongation and weakening of Si(Hf)—O bonds which facilitates the thermally activated formation of Frenkel defects: neutral O vacancies and interstitial O^{2-} ions. However, the barriers for these processes are quite different. In a-SiO_2 the barrier for formation of a neutral O vacancy and interstitial O^{2-} ion is on average 0.7 eV [8] whereas in a-HfO_2 it is much higher at about 2 eV [30]. These barriers depend on local environment of a particular site and are distributed within 0.5 eV. O^{2-} ions are very mobile in both cases with the average barriers for diffusion of 0.3 eV and 0.5 eV in a-SiO_2 and HfO_2, correspondingly [8,29].

V. Comparison with experimental data and impact of electron-assisted bond breakage on SiO_2 TDDB statistics

Directly proving the validity of these mechanisms in thin oxide films is difficult due to insufficient sensitivity of spectroscopic methods, while electron and hole trapping in bulk silica glass have been studied more thoroughly. Electrons and holes can be produced by irradiation of glass samples. Recently it has been demonstrated that the electron traps described above can be responsible for the optical absorption bands peaking at 3.7 eV, 4.7 eV, and 6.4 eV in SiO_2 glass samples irradiated by electrons at 80 K [31].

The feasibility of the breakdown mechanism based on Frenkel defects creation facilitated by electron injection in a-SiO_2 has been tested in ref. [32]. The multiscale model proposed in this work self-consistently describes the main physical mechanisms in SiO_2 subjected to an electrical stress using the parameters generated by DFT calculations that explicitly consider SiO_2-specific defect characteristics and defect generation mechanisms. Charge transport is modelled self-consistently by including direct tunneling, defect assisted multi-phonon Trap-Assisted-Tunneling (TAT) [33], and carrier drift across either the conduction, valence or defect sub-bands. The defect properties predicted from DFT were then used to

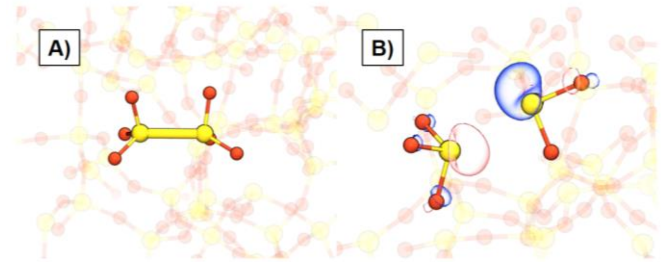

Figure 3. A) A typical O vacancy configuration in a-SiO_2. B) The same O vacancy with two trapped electrons. The Si atoms within the vacancy pivot to point away from each other. Si atoms are shown in yellow while O atoms are shown in red. An iso-surface of the HOMO is shown in blue and pink.

calculate TAT current contributions while accounting for electron-phonon coupling. Electron trapping sites were randomly and uniformly generated in simulated samples with the energy parameters within the energy ranges reported in [8,22,34]. The time-dependent dielectric breakdown (TDDB) distributions were then simulated at different stress voltages. The good agreement between simulations and experiments obtained in [32] at different biases confirmed that this mechanism could be responsible for the degradation and dielectric breakdown in silica. However, a more accurate model should account for correlation in defect creation, i.e. processes by which pre-existing vacancies affect the formation of new vacancies.

VI. CORRELATION EFFECTS IN DEFECT CREATION

As explained above, a-SiO_2 and a-HfO_2 have differing concentrations and energy depths of trapping sites. In the following, we will therefore address them separately.

A. *Correlated defect creation in SiO_2*

In a-SiO_2, the structural precursors for electron trapping are further apart but barriers for defect creation from bi-polaron states are lower than in a-HfO_2, where the density of electron trapping sites is much higher. The cost of creating an oxygen vacancy depends greatly on the local environment. Not only is there a spread of formation energies owing to the disorder, but pre-existing vacancies can affect both the position and the barrier for forming a new vacancy. The presence of an existing vacancy close to the bi-polaron may either facilitate or hinder the next vacancy-creation process.

This can manifest in several ways: i) electron trapping in a vacancy in the course of TAT can facilitate the formation of a new vacancy nearby; ii) the distortion of the surrounding network caused by electron trapping in a vacancy can create another precursor site for electron trapping nearby; iii) the aggregation of several vacancies can distort the surrounding network and enhance local electric field, leading to creation of new vacancies. In all cases the number of O vacancies grows with increasing degradation of the film.

In a-SiO_2 the O vacancy can trap two electrons and the charge transition levels that correspond to O vacancies are favorably positioned to participate in TAT. When two electrons localize onto an O vacancy, the defect distorts as the two 3-coordinated Si atoms shift to point away from each other, as shown in Fig. 3. The highest occupied molecular orbital (HOMO) of a negatively charged O vacancy is shown in Fig. 3B. As a result of this distortion, there is a small chance that one of the lobes of the HOMO will point directly at a neighboring 4-coordinated Si atom.

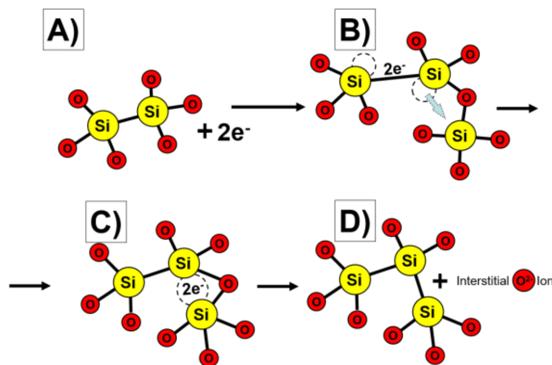

Figure 4. Schematic illustrating the correlated defect creation mechanism. A) O Vacancies can trap up to two electrons; and B) distort the amorphous structure. C) In rare cases, the HOMO of the charged vacancy points towards a neighbouring Si atom and forms a bond to D) create a new vacancy and interstitial O.

To determine the likelihood of creating another O vacancy near an existing one, 144 possible vacancy geometries were investigated. In 97% of these geometries, the vacancy simply trapped two electrons by distorting, as shown in Fig. 3 and Fig. 4B. In two rare cases the HOMO happened to point at a neighboring 4-coordinated Si atom, as shown in Fig. 4C. This configuration facilitates the creation of another O vacancy and O interstitial ion through a process with an average barrier of 1.1 eV. A schematic of this correlated defect creation mechanism is shown in Fig. 4A-D. However, the probability of this process occurring is only about 3%.

Another possibility is that new intrinsic wide-angle electron trapping sites are created when O vacancies take part in TAT and are occupied by electrons. Creation of these traps is directly related to the local strain present in the system and both the creation of vacancies and the localization of electrons results in an increase of local strain. To examine this effect, extra electrons were injected into newly formed O vacancies. After the geometry of the doubly negatively charged O vacancy was relaxed, another electron was added into the system to test whether precursor sites for electron trapping were created. Out of a total of 142 geometries (excluding the two examples of correlated defect creation) a new wide angle intrinsic trapping site was found 38 times. In these examples two electrons first localized onto the O vacancy and additional electrons were then able to access a newly created wide O-Si-O bond angle site nearby created by the network distortion induced by the vacancy relaxation. The probability of creating these new precursor sites is about 25%. Trapping two electrons at these new precursor sites generates new O vacancies and interstitial O^{2-} ions, as described above.

Since creation of additional wide O-Si-O angle intrinsic electron traps is associated with the local strain due to the presence of defects, it is natural to expect that increasing the concentration of defects should increase the probability of generating new precursor sites for electron trapping. As additional vacancies are created near pre-existing ones, the amount of local strain produced increases as well. To investigate this effect, we examined 40 divacancy

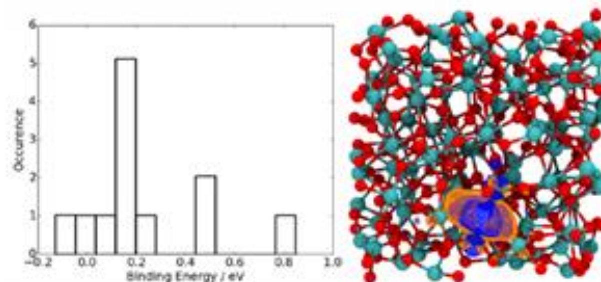

Figure 5. Left: Histogram of the binding energies for di-vacancies in a-HfO_2. A total of 12 configurations were calculated. Positive binding energies indicate 'attraction' between vacancies, whereas negative binding energies indicate repulsion. Right: A typical oxygen di-vacancy configuration for a-HfO_2. Red indicates oxygen and cyan indicates hafnium ions. Wire mesh surfaces are iso-surfaces of the square moduli of the two (double occupied) di-vacancy states. The states are extended across both of the vacancies, indicating binding between the vacancies.

geometries containing 214 atoms each and observed that in 20 cases wide O-Si-O bond angle sites were created due to electron trapping at vacancies. This demonstrates that indeed aggregation of O vacancies and TAT through them increases

the probabilities of creating new vacancies nearby and that of growing new vacancy clusters.

We further investigated this trend by examining whether O tri-vacancies will also induce wide O-Si-O angle precursor sites. To accommodate such large defect clusters, we created a library of 648-atom a-SiO_2 cells using the melt and quench procedure described in [22]. These larger amorphous structures were then screened for existing defects or wide angle intrinsic traps and 5 defect-free geometries were selected. Using these large cells, three libraries of tri-vacancy geometries were created to account for the more variable structure of these larger clusters. The first set of tri-vacancy geometries consisted of examples where the three defects were tightly clustered. The second set was composed of examples where the three defects were arranged in a linear array. Finally, in the third set of geometries each contained three loosely associated vacancies within two nearest neighbor sites of each other. Ten geometries from each set were selected for analysis at random and each of them was simulated with 1 to 7 extra electrons in the system. In 23 out of 30 geometries, strain induced wide O-Si-O angle intrinsic traps were observed after the pre-existing vacancies were charged. These newly created intrinsic traps were evenly distributed between the three types of tri-vacancy geometries, indicating that their exact configuration does not have a large effect on the correlated creation of new defects.

These results suggest that, as the size of O vacancy clusters increases, the likelihood of creating another vacancy nearby increases as well. Single vacancies have a 25% chance of inducing a wide O-Si-O angle intrinsic electron trap when charged, divacancies have a 50% chance, and tri-vacancies are the most likely to create a nearby intrinsic trap with a 77% chance.

B. *Correlated defect creation in HfO_2*

As described above, the electron trap density in a-HfO_2 is much higher than in a-SiO_2 with an average distance between precursor sites about 8 Å, which corresponds to a density of $\sim 2 \cdot 10^{21}$ cm^{-3}. However, not all of the traps can trap electrons efficiently, i.e. by tunneling from substrate, as some of the traps are higher in energy than others by as much as 0.5 eV. Therefore, it is of interest to find out whether there is another mechanism for generating more O vacancies when electron trapping precursor sites are converted into O vacancies.

One such a mechanism was suggested for m-HfO_2 in [29] and also involves trapping of two electrons at a pre-existing neutral O vacancy. In both m-HfO_2 and a-HfO_2 electrons trapped by O vacancy have polaronic nature and occupy relatively shallow electronic states in the gap [35]. DFT calculations show that, when an O vacancy traps two extra electrons, the formation energy of the second vacancy produced at the nearest neighbor position is lower than that for the first one. This results from attraction between the vacancies.

To study how the interaction between vacancies depends on their mutual position in a-HfO_2, we performed calculations for 12 different configurations. Di-vacancy configurations were produced by first taking a set of four 'parent' vacancies. Then, for each parent three di-vacancies were produced by deleting adjacent oxygen atoms. The four parent vacancies were all at 3-coordinated oxygen sites and were chosen to be representative of the average isolated vacancy. The choice of the original set of parent vacancies should not, however, greatly affect the results as the formation energy distribution for neutral oxygen vacancies is in any case very narrow (approximately 0.2 eV). Fig. 5 shows the distribution of binding energies of oxygen vacancies in a-HfO_2.

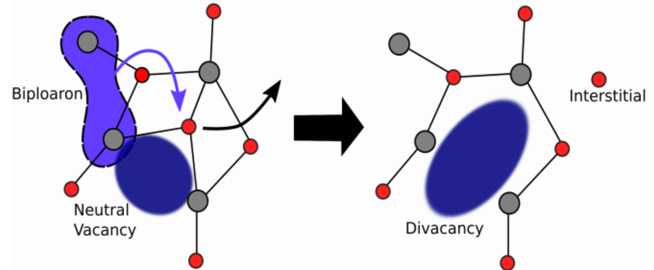

Figure 6. Schematic of the Frenkel pair formation mechanism in a-HfO_2. Red indicates oxygen and grey Hafnium. A bi-polaron trapped on or adjacent to an oxygen vacancy lowers the barrier to form an O vacancy and O^{2-} interstitial pair, similar to the mechanism for the creation of isolated Frenkel pairs [29,30]. The cost to create the di-vacancy, however, is lower. This explains the correlation effects seen in a-HfO_2 conductive filament formation.

Vacancies are said to be 'binding' if the total energy of the system is lower when they are in close proximity to each other than if they are apart. Positive energies indicate vacancy attraction, whereas negative values of a binding energy indicate repulsion. The binding energies are widely distributed with some individual values indicating weak vacancy-vacancy repulsion. However, the average binding energy across the sample is approximately 0.2 eV, suggesting that the formation energy of a new neutral vacancy (next to a pre-existing one) will on average cost 0.2 eV less than the creation of a single, isolated vacancy. The wide distribution of the binding energies indicates that there will be some di-vacancy configurations which are strongly bound and thus very energetically favorable. One configuration, for example, has a binding energy of 0.8 eV. A typical di-vacancy configuration in a-HfO_2 is shown on the right panel of Fig. 5. Interaction between the vacancies is visualized by the plot of the di-vacancy doubly occupied electron state. Instead of two localized states adjacent to one another, the plot shows two states which are extended across the vacancies in a bond-like fashion.

The correlation effect in O vacancy formation in a-HfO_2 is explained schematically in Figure 6. It shows a doubly negatively charged O vacancy on the left transforming into a di-vacancy and an interstitial O^{2-} ion on the right. The energy cost of creating the second O vacancy is reduced by the presence of a nearby vacancy. Therefore, the trapping of bi-polarons onto O vacancies will be involved in the creation of Frenkel pairs at a lower energetic cost when compared to the creation of isolated defects.

VII. CONCLUSIONS

We presented the mechanisms of defect formation in a-SiO_2 and a-HfO_2 which can contribute to initial stages of degradation of these films under bias application in electronic

devices. The results demonstrate that breaking Si-O bonds and formation of O vacancies and O atom interstitials as a result of thermal activation and bias application is energetically unfeasible in the perfect network, in contrast with the predictions of the thermochemical E model. Electrons injected either by the Fowler-Nordheim tunneling or by direct tunneling into the structural trapping sites can weaken Si(Hf)-O bonds that the thermally activated creation of Frenkel defects, O vacancies and O^{2-} interstitial ions, becomes efficient even at room temperature when two electrons are trapped at the same site. However, the number of such traps is limited and other processes for generating more O vacancies when all original electron trapping precursor sites are exhausted should be involved to explain oxide degradation and breakdown.

We demonstrate that trapping two electrons at O vacancy sites in a-SiO_2 induces local distortion in the amorphous network such that new O-Si-O precursor sites for electron trapping are created with the probability of about 25%. These sites can trap two extra electrons producing a new vacancy nearby. As the size of the O vacancy clusters increases, the

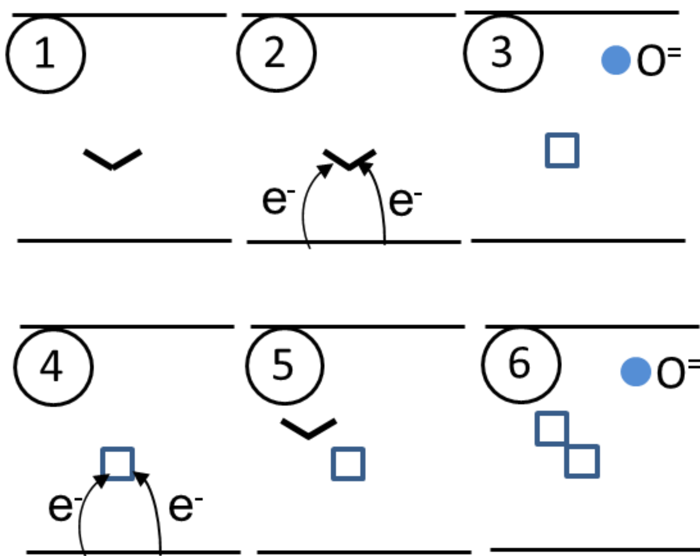

Figure 7. Schematic of the proposed degradation mechanism in a-SiO_2 and a-HfO_2 facilitated by electron injection. (1) Shows an electron trap in amorphous structure; in (2) this trap captures two electrons from the substrate, which results in the formation of Frenkel defects in (3). In (4) two electrons are trapped on O vacancy; this creates an electron trap nearby in (5) and the formation of another O vacancy and interstitial O^{2-} ion in (6). Further trapping of electrons results in the formation of more O vacancies nearby, as discussed in VIA.

likelihood of creating another vacancy nearby increases as well. Di-vacancies have a 50% chance, and tri-vacancies are the most likely to create a nearby intrinsic trap with a 77% chance. We demonstrate that a similar mechanism can produce new vacancies at pre-existing vacancies also in a-HfO_2. In this case, two electrons trapped at a pre-exiting vacancy directly facilitate the formation of a new vacancy and an interstitial O^{2-} ion rather than produce a new electron trapping site nearby. However, the energy barriers for defect creation in a-SiO_2 are much lower than those in a-HfO_2. These results suggest that, although the mechanisms of O vacancy creation in amorphous SiO_2 and HfO_2 are similar, correlation effects in the time to breakdown statistics of a-SiO_2 and a-HfO_2 films should be different. This degradation process is schematically summarized in Fig. 7.

The microscopic mechanisms responsible for the creation of O vacancies and the related correlation effect strongly affect the BD and TDDB statistics. Using the multi-scale modeling platform presented in [32] allows investigating the impact of the defect correlation on TDDB distribution. One of the most significant results of this study is that increasing the correlation of the defect creation process reduces the dependence of the Weibull slope (β) of TDDB distribution on the layer thickness (t_{ox}). This finding explains the experimental trend observed on β-t_{ox} curves observed on SiO_2 and high-k dielectrics, as explained in [36].

ACKNOWLEDGEMENT

We acknowledge funding provided by the UK Engineering and Physical Sciences Research Council (EPSRC) under grants No. EP/K01739X/1 and EP/P013503/1 and by the Leverhulme Trust RPG-2016-135. J.S. is funded by EPSRC grant no. EP/G036675/1 to the Center for Doctoral Training. Computer facilities on Archer service have been provided via the UKs HPC Materials Chemistry Consortium (EPSRC Grant No. EP/L000202).

REFERENCES

[1] S. Lombardo, J.H. Stathis, B.P. Linder, K.L. Pey, F. Palumbo, and C.H. Tung, "Dielectric breakdown mechanisms in gate oxides,". *J Appl. Phys.*, vol. 98, p. 121301, 2005.

[2] S. Mukhopadhyay, P.V. Sushko, A.M. Stoneham, and A.L. Shluger, "Correlation between the atomic structure, formation energies, and optical absorption of neutral oxygen vacancies in amorphous silica," *Phys. Rev. B,* vol. 71, p. 235204, 2005.

[3] X. Li, C. H. Tung and K.- L. Pey, "The radial distribution of defects in a percolation path," *Appl. Phys. Lett.* vol. 93, pp. 262902, 2009.

[4] A. Mehonic, M. Buckwell, L. Montesi, M. S. Munde, D. Z. Gao, S. Hudziak, R. J. Chater, S. Fearn, D. McPhail, M. Bosman, A. L. Shluger, and A. J. Kenyon, "Nanoscale Transformations in Metastable, Amorphous, Silicon-Rich Silica," *Adv. Mater,* vol.. 28, pp. 7486, 2016.

[5] J. Yao, L. Zhong, D. Natelson and J. M. Tour, "In situ imaging of the conducting filament in a silicon oxide resistive switch," *Sci. Rep.* vol. 2, pp. 242, 2012.

[6] Y. Wang, Q. Xinye, K. Chen, Z. Fong, W. Li and J. Xu, "Resistive switching mechanism in silicon highly rich SiOx (x<0.75) films based on silicon dangling bonds percolation model," *Appl. Phys. Lett.* vol. 102, pp. 042103, 2013.

[7] A. Mehonic, S. Cueff, M. Wojdak, S. Hudziak, O.Jambois, C. Labbé, B. Garrido, R. Rizk R and A. J. Kenyon, "Resistive switching in silicon suboxide films," *J. Appl.Phys.* vol. 111, 074507, 2012.

[8] D. Z. Gao, A.-M. El-Sayed and A. L. Shluger, "A mechanism for Frenkel defect creation in amorphous SiO_2 facilitated by electron injection," *Nanotechnology*, vol. 27, pp. 505207-7, 2016.

[9] M. S. Munde, D. Z. Gao and A. L. Shluger, "Diffusion and aggregation of oxygen vacancies in amorphous silica," *J. Phys. Condens. Matter,* vol. 29, pp. 245701-10, 2017.

[10] S. R. Bradley, G. Bersuker, and A. L. Shluger, "Modelling of oxygen vacancy aggregatesin monoclinic HfO_2: can they contribute to conductive filament formation?" *J. Phys.: Condens. Matter*, vol. 27, pp. 415401, 2015.

[11] G. Broglia, G. Ori, L. Larcher and M Montorsi, "Molecular dynamics simulation of amorphous HfO_2 for resistive RAM applications," *Modelling and Simul. Mater. Sci. Eng.*, vol. 22, pp. 065006, 2014.

[12] J. C. Fogarty, H. M. Aktulga, A. Y. Grama, A. C. T. van Duin, and S. A. Pandit, "A reactive molecular dynamics simulation of the silica-water interface," *J. Chem. Phys.* , vol. 117, pp. 174704, 2010.

[13] S. Plimpton, "Fast Parallel Algorithms for Short-Range Molecular Dynamics," *J. Comput. Phys.* vol. 117, pp. 1, 1995.

[14] J. VandeVondele, M. Krack, F. Mohamed, M. Parrinello, T. Chassaing, J. Hutter, "Quickstep: Fast and accurate density functional calculations using a mixed Gaussian and plane waves approach," *Comput. Phys. Commun.*, vol. 167, pp. 103-128, 2005.

[15] M. Guidon, J. Hutter, J. VandeVondele, "Robust Periodic Hartree− Fock Exchange for Large-Scale Simulations Using Gaussian Basis Sets," *J. Chem. Theory Comput.*, vol. 5, pp. 3010-3021, 2009.

[16] M. Guidon, J. Hutter, J. VandeVondele, "Auxiliary Density Matrix Methods for Hartree− Fock Exchange Calculations," *J. Chem. Theory Comput.* vol. 6, pp. 2348–2364, 2010.

[17] J. VandeVondele, J. Hutter, "Gaussian basis sets for accurate calculations on molecular systems in gas and condensed phases," *J. Chem. Phys.*, vol. 127, pp.114105–1–9, 2007.

[18] S. Goedecker, M. Teter, J. Hutter, "Separable dual-space Gaussian pseudopotentials," *J. Phys. Rev. B*, vol. 54, pp. 1703−1710, 1996..

[19] M. Krack, "Pseudopotentials for H to Kr optimized for gradient-corrected exchange-correlation functionals," *Theor. Chem. Accounts*, vol. 114, pp. 145-152, 2005.

[20] Sanliang Ling, private communications.

[21] M. Guidon, J. Hutter, and J. VandeVondele, "Robust Periodic Hartree-Fock Exchange for Large-Scale Simulations Using Gaussian Basis Sets," *J. Chem. Theory Comput.* vol. 5, pp 3010, 2009.

[22] A-M. El-Sayed, M. B. Watkins, V. V. Afanas'ev, and A. L. Shluger, "Nature of intrinsic and extrinsic electron trapping in SiO_2," *Phys, Rev. B* vol. 89, pp. 125201, 2014.

[23] M. Kaviani, J. Strand, V. V. Afanas'ev, and A. L. Shluger, "Deep electron and hole polarons and bipolarons in amorphous oxide," *Phys. Rev.* B, vol. 94, pp. 020103(R), 2016.

[24] J. Strand, M. Kaviani, V. V. Afanas'ev, J. G. Lisoni, and A. L. Shluger, "Intrinsic electron trapping in amorphous oxides," *Nanotechnology* (accepted).

[25] J. McPherson, J. Y. Kim, A. Shanware, and H. Mogul, "Thermochemical description of dielectric breakdown in high dielectric constant materials," *Appl. Phys. Lett.* vol. 82, pp. 2121, 2003.

[26] J. W. McPherson, "Extended Mie-Grüneisen molecular model for time dependent dielectric breakdown in silica detailing the critical roles of O–$Si{\equiv}O_3$ tetragonal bonding, stretched bonds, hole capture, and hydrogen release," *J. Appl. Phys.*, vol. 99, pp. 083501, 2006.

[27] J. W. McPherson, "Quantum Mechanical Treatment of Si-O Bond Breakage in Silica Under Time Dependent Dielectric Breakdown Testing," 2007 IEEE International Reliability Physics Symposium Proceedings. 45th Annual, pp. 209-216 (2007)

[28] N. A. Spaldin, "Beginner's Guide to the Modern Theory of Polarization," *J. Sol. State. Chem.*, vol. 195, pp. 2-22, 2012.

[29] S. R. Bradley and A. L. Shluger, "Electron-Injection-Assisted Generation of Oxygen Vacancies in Monoclinic HfO_2," *Phys. Rev. Appl.*, vol. 4, pp. 064008, 2015.

[30] J. Strand, M. Kaviani, A. L. Shluger, "Defect creation in amorphous HfO_2 facilitated by hole and electron injection," *Microel. Eng.* vol. 178, pp. 279-283, 2017.

[31] A-M. El-Sayed, K. Tanimura, and A. L. Shluger, "Optical signatures of intrinsic electron localization in amorphous SiO_2," *J. Phys.: Condens. Matter* **27**, pp. 265501, 2015.

[32] A. Padovani, D. Z. Gao, A. L. Shluger, and L. Larcher, "A microscopic mechanism of dielectric breakdown in SiO_2 films: An insight from multi-scale modeling," *J. Appl. Phys.* vol. 121, pp. 155101-10, 2017.

[33] L. Vandelli, A. Padovani, L. Larcher, R.G. Southwick, W.B. Knowlton, and G. Bersuker, "A Physical Model of the Temperature Dependence of the Current Through Stacks," *IEEE Transactions on Electron Devices* vol. 58, pp. 2878-2887, 2011.

[34] A Kimmel, P Sushko, A Shluger, G Bersuker, "Positive and negative oxygen vacancies in amorphous silica," *ECS Transactions*, vol. 19, pp. 3-17, 2009.

[35] D. Muñoz Ramo, J. L. Gavartin, A. L. Shluger, and G. Bersuker, "Spectroscopic properties of oxygen vacancies in monoclinic HfO2 calculated with periodic and embedded cluster density functional theory," *Phys. Rev.* B, vol. 75, pp. 205336, 2007.

[36] A. Padovani and L. Larcher, "Time-Dependent Dielectric Brekdown Statistics in SiO_2 and HfO_2 Dielectrics: Insights from a Multi-Scale Modeling Approach," to be presented at IRPS 2018